TeV gamma-rays from photo-disintegration/de-excitation of nuclei in Westerlund 2

LUIS A. ANCHORDOQUI[1], JOHN F. BEACOM[2], YOUSAF M. BUTT[3], HAIM GOLDBERG[4], SERGIO PALOMARES-RUIZ[5], THOMAS J. WEILER[6], AND JUSTIN WESOLOWSKI[1]
[1]*Department of Physics, University of Wisconsin-Milwaukee, Milwaukee, WI 53201*
[2]*Departments of Physics and Astronomy, The Ohio State University, Columbus, OH 43210*
[3]*Harvard-Smithsonian Center for Astrophysics, 60 Garden St., Cambridge, MA02138*
[4]*Department of Physics, Northeastern University, Boston, MA 02115*
[5]*IPPP, Department of Physics, University of Durham, DH1 3LE UK*
[6]*Department of Physics and Astronomy, Vanderbilt University, Nashville, TN 37235*
t.weiler@vanderbilt.edu

Abstract: TeV gamma-rays can result from the photo-de-excitation of PeV cosmic ray nuclei after their parents have undergone photo-disintegration in an environment of ultraviolet photons. This process is proposed as a candidate explanation of the recently discovered HESS source at the edge of Westerlund 2. The UV background is provided by Lyman-alpha emission within the rich O and B stellar environment. The HESS flux results if there is efficient acceleration at the source of lower energy nuclei. The requirement that the Lorentz-boosted ultraviolet photons reach the Giant Dipole resonant energy ($\sim$ 20 MeV) implies a strong suppression of the gamma-ray spectrum compared to an E_γ^{-2} behavior at energies below about 1 TeV. This suppression is not apparent in the lowest-energy Westerlund 2 datum, but will be probed by the upcoming GLAST mission.

Two well-known mechanisms for generating TeV γ-rays in astrophysical sources are the purely electromagnetic (EM) synchrotron emission and inverse Compton scattering, and the hadronic (PION) one in which γ-rays originate from π^0 production and decay. Very recently, we highlighted a third dynamic which leads to TeV γ-rays: photo-disintegration of high-energy nuclei, followed by immediate photo-emission from the excited daughter nuclei [1]. For brevity, we label the photo-nuclear process $A + \gamma \to A'^* + X$, followed by $A'^* \longrightarrow A' + \gamma$-ray as "$A^*$". Such a process may be operative in massive star formation regions with hot starlight. In this work we examine whether the A^*-process could be the origin of the very energetic γ-rays recently observed, with the High Energy Stereoscopic System (HESS) of Atmospheric Cherenkov Telescopes, from the young stellar cluster Westerlund 2 [2].

RCW 49 is a luminous cloud of ionized hydrogen located towards the outer edge of the Carina arm, at a distance $d \approx 8$ kpc [3]. Embedded in RCW 49 is the massive star formation region Westerlund 2, hosting an extraordinary ensemble of hot OB stars; presumably at least a dozen early-type O stars, 100 B stars, and the remarkable Wolf-Rayet binary WR 20a [4]. For such a distance, the cluster core $\sim 5'$ results in a physical extent $R \sim 6$ pc. The total mass of the stars within this region is found to be $\approx 4500\, M_\odot$. The total wind luminosity of all these O type stars has been estimated as $\sim 5 \times 10^{37}$ erg s^{-1}, and the stellar luminosity of known massive stars is $L = 2.15 \times 10^{40}$ erg s^{-1} [5]. However, radio emission from the prominent giant HII region RCW 49 requires a larger luminosity of ionizing UV photons [6]. Indeed observations using the Infrared Array Camera (IRAC) on board the Spitzer Space Telescope indicate that the total number of young stellar objects in this region is about 7000 [7]. Therefore, the above estimate of the total stellar luminosity should be taken as a lower bound.

In the vicinity of WR20a, a clear excess of very high energy γ-rays was recently reported by the

H.E.S.S. Collaboration [2]. The significance of the excess is about 9σ. Compared to the point spread function of the instrument, the source (termed HESS J1023–2013575) appears slightly extended, corresponding to an intrinsic size of the γ-ray source of about $0.2°$; its center is slightly shifted compared to WR 20a. As expected for an extended source, the γ-ray flux is steady over time.

By repeating the discussion of Cygnus OB2 [8], in what follows we obtain the expected γ-ray production through the A^*-process in Westerlund 2. To compute the photo-disintegration rate of a highly relativistic nucleus (with energy $E = A E_N = \gamma A m_N$, where γ is the Lorentz factor) on starlight per nucleon [9],

$$R_A(E_N) = \frac{c}{\lambda_A} \approx \frac{\pi\, \sigma_0\, \epsilon_0'\, \Gamma}{4\gamma^2} \int_{\epsilon_0'/2\gamma}^{\infty} \frac{d\epsilon}{\epsilon^2}\; n(\epsilon)\,, \tag{1}$$

we must estimate the ambient photon distribution with energy spectrum $n(\epsilon)$. In Eq. (1) we have approximated the Giant Dipole resonant cross section by the single pole of the Narrow-Width Approximation,

$$\sigma_A(\epsilon') = \pi\; \sigma_0\; \frac{\Gamma}{2}\; \delta(\epsilon' - \epsilon_0')\,. \tag{2}$$

Here, ϵ' is the photon energy in the rest frame of the nucleus, $\sigma_0/A = 1.45 \times 10^{-27}\mathrm{cm}^2$, $\Gamma = 8$ MeV, and $\epsilon_0' = 42.65 A^{-0.21}\,(0.925 A^{2.433})$ MeV, for $A > 4$ ($A \leq 4$). The ambient photon distribution originates in the thermal emission of the stars in the core region of radius R. The average density in the region R will reflect both the temperatures $T_{\rm O}$ and $T_{\rm B}$ due to emission from O and B stars, respectively, and the dilution resulting from inverse square law considerations. Specifically, the photon density is

$$n(\epsilon) = \frac{9}{4}\left[\frac{n_{\rm O}(\epsilon) N_{\rm O} R_{\rm O}^2 + n_{\rm B}(\epsilon) N_{\rm B} R_{\rm B}^2}{R^2}\right], \tag{3}$$

where $N_{\rm O\,(B)}$ is the number of O (B) stars , $R_{\rm O(B)}$ is the O(B) star average radius, the factor 9/4 emerges when averaging the inverse square distance of an observer from uniformly distributed sources in a region R, and

$$n_{\rm O(B)}(\epsilon) = (\epsilon/\pi)^2\; \left[e^{\epsilon/T_{\rm O(B)}} - 1\right]^{-1}\,, \tag{4}$$

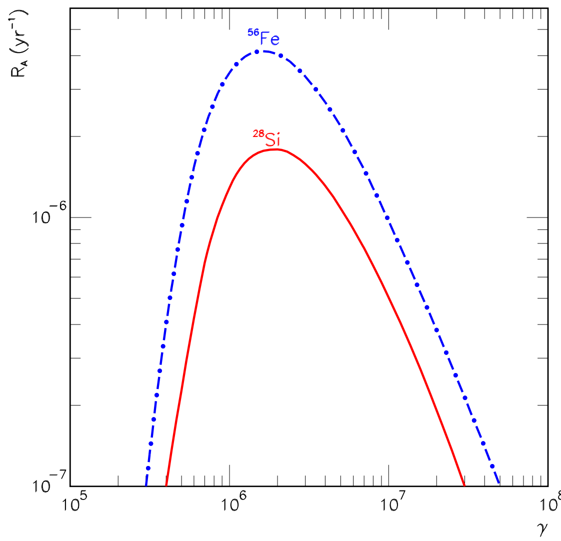

Figure 1: Photo-disintegration rates of ^{56}Fe and ^{28}Si, on the Westerlund 2 starlight.

corresponding to a Bose-Einstein distribution with temperature $T_{\rm O(B)}$.

In Fig. 1 we show the dependence on the Lorentz factor of R_{56} and R_{28} for the stellar ambiance described above. We have taken for the O stars, $N_{\rm O} = 12$, a surface temperature T_O = 40000 K, and radius $R_O = 19\ R_\odot$; for the cooler B stars we assign T_B = 18000 K, $N_{\rm B} = 100$, and radius $R_B = 8\ R_\odot$.

The low energy cutoff on R_A seen in Fig. 1 will be mirrored in the resulting photon distribution. The $\sim E^{-2}$ energy behavior of the various nuclear fluxes will not substantially affect this low energy feature. The energy behavior for photons in the $0.5 - 10$ TeV region of the HESS data is a complex convolution of the energy distributions of the various nuclei participating in the photo-disintegration, with the rate factors appropriate to the eV photon density for the various stellar populations.

Let us define the differential rate dR_A/dE_γ' as

$$\frac{dR_A}{dE_\gamma'} = \frac{1}{2}\int_0^{\infty} \frac{n(\epsilon)}{\gamma^2\epsilon^2}\, d\epsilon \times \int_0^{2\gamma\epsilon} \epsilon'\, \frac{d\sigma_{\gamma A}}{dE_\gamma'}(\epsilon', E_\gamma')\, d\epsilon'\,, \tag{5}$$

where $d\sigma_{\gamma A}(\epsilon', E'_\gamma)/dE'_\gamma$ is the inclusive differential cross section for production of γ-rays from disintegration and E'_γ is the energy of the emitted photon(s) in the rest frame of the nucleus. Assuming the same cosmic ray spectrum as above, the emissivity (number/volume/steradian) of γ-rays coming from nuclei photo-emission is

$$Q_\gamma^{\rm dis}(E_\gamma) = \sum_A \int \frac{dn_A}{dE_N}(E_N)\, dE_N \times \int \frac{dR_A}{dE'_\gamma}\, dE'_\gamma\, \frac{d\cos\theta_\gamma}{2} \times \delta[E_\gamma - \gamma E'_\gamma(1+\cos\theta_\gamma)] \;, \quad (6)$$

where E_γ is the energy of the emitted γ-ray in the lab and θ_γ is the γ-ray angle with respect to the direction of the excited nucleus. Assuming a power law with spectral index α for the nuclear flux, and approximating the γ-ray spectrum as being monochromatic with energy $\overline{E'_{\gamma A}}$, the emissivity becomes [10]

$$Q_\gamma^{\rm dis}(E_\gamma) = \sum_A \frac{\overline{n_A} m_N}{2\overline{E'_{\gamma A}}} \int_{\frac{m_N E_\gamma}{2\overline{E'_{\gamma A}}}} \frac{dE_N}{E_N} \times R_A(E_N)\, \frac{dn_A}{dE_N}(E_N)\,, \quad (7)$$

where $\overline{n_A}$ is the mean γ-ray multiplicity for a nucleus with atomic number A. (Hereafter we take $\overline{n_A} = 2$). The differential flux at the observer's site (assuming there is no absorption) is related to to the γ-ray emissivity as

$$\frac{dF_\gamma}{dE_\gamma}(E_\gamma) = \frac{V_{\rm dis}}{4\pi d^2}\, Q_\gamma^{\rm dis}(E_\gamma)\,, \quad (8)$$

where $V_{\rm dis}$ is the volume of the source (disintegration) region and d is the distance to the observer.

In Fig. 2 we provide a sample of eyeball fits to the gamma ray spectrum, as obtained following a direct integration of Eq. (7). The fits are for interesting choices of the spectral index (α) of the nuclei population and for the average energy of the photon (in the nuclear rest frame) emitted during photo-emission. It is apparent that the A* mechanism can provide reasonable agreement with the data, except possibly for the lowest-energy datum. This datum may require an alternate mechanism, such as electron acceleration or a PION contribution [11].

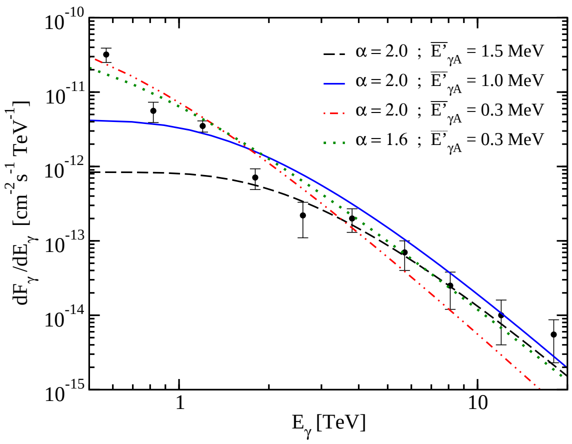

Figure 2: Sample eyeball fits to HESS Westerlund 2 γ-ray spectrum for the A^* model, with various values of the injection ^{56}Fe nuclei power index α and the average energy $\overline{E'_{\gamma A}}$ of emitted de-excitation photons.

The EM and PION pp processes contrast with the A^*-process in that for them there is either no energy threshold (EM) or very small threshold $\mathcal{O}(2m_\pi)$ (PION pp) in the lab, and so their resulting γ-ray spectra rise monotonically with decreasing E_γ. In contrast, the A^* spectrum is flat with decreasing E_γ below about a TeV, as is evident in Fig. 2.

The conversion efficiency from cosmic-rays to TeV γ-rays must be quite high in the A^* model, as with other models. We find that the ratio of power in the nuclei flux to that in the O-star winds is

$$\frac{P_A}{P_{\rm O\ wind}} = {\rm eff} \times \left(\frac{R}{6\,{\rm pc}}\right)^2 \left(\frac{d}{8\,{\rm kpc}}\right)^2 \times \left(\frac{40}{N_{\rm O}}\right)^2 \left(\frac{\tau_{\rm age}}{\tau_{\rm cont}}\right) \quad (9)$$

where eff is an efficiency which depends on model parameters, $\tau_{\rm age} \sim 2\,{\rm Myr}$ is the age of the star-forming region [5], and $\tau_{\rm cont}$ is the containment time of the nuclei in the ambient magnetic field. For the four parameter sets $(\alpha, \overline{E'_{\gamma A}}/{\rm MeV})$ listed in Fig. 2, we find for the (2.0, 1.5), (2.0, 1.0), (1.6, 0.3) and (2.0, 0.3) models, the respective efficiency values of ${\rm eff} = 4\%$, 8%, 20%, and 80%.

In summary, we have shown that the observed TeV γ-rays from Westerlund 2 can be explained by the A^* model, wherein the TeV γ-rays are the Lorentz-boosted MeV γ-rays emitted on the de-excitation of daughter nuclei, themselves produced in collisions of PeV nuclei with a hot ultraviolet photon background. There is a specific prediction of a suppression of the γ-ray spectrum in the region below $1\ \mathrm{TeV}$ – this because of the need to achieve Giant Dipole Resonance excitation through collision with $\sim$ few eV photons. This suppression is not apparent in the lowest-energy Westerlund 2 datum, but will be probed by the upcoming GLAST mission [12]: The flux predicted at $\sim$ 100 GeV from an $E_\gamma^{-2.53}$ extrapolation of the HESS data [2] would render the source spectacularly visible in the GLAST observation, whereas the A^*-model predicts a suppression by a factor of more than 2 orders of magnitude relative to this extrapolated flux.

We have also calculated the energy requirements for the proposed mechanism by integrating over the nuclei energy density. We have found that, in order to fall within the estimated kinetic energy budget of the O stars, the containment time needs to be large (of $\mathcal{O}(10^5 \mathrm{yr})$), so that the wind power integrates in time to a sufficiently large energy. It should be noted that WR 20a may by itself contribute several times the wind energy of the O stars, thereby lowering our effeciency factor by a comparable amount.

The research of JFB is supported by The Ohio State University and the NSF CAREER Grant No. PHY-0547102. YMB is supported by NASA/Chandra and NASA/INTEGRAL GO Grants and a NASA LTSA Grant. HG is supported by the U.S. NSF Grant No PHY-0244507. SPR is partially supported by the Spanish Grant FPA2005-01678 of the MCT. TJW is supported by the U.S. DOE Grant No. DE-FG05-85ER40226. HG, SPR, and TJW thank the Aspen Center for Physics for a productive environment during this work.

References

[1] L. A. Anchordoqui, J. F. Beacom, H. Goldberg, S. Palomares-Ruiz and T. J. Weiler, Phys. Rev. Lett. **98**, 121101 (2007) [arXiv:astro-ph/0611580].

[2] F. Aharonian [H.E.S.S. Collaboration], Astron. Astrophys. **467**, 1075 (2007) [arXiv:astro-ph/0703427].

[3] G. Rauw *et al.*, Astron. Astrophys. **463**, 981 (2007) [arXiv:astro-ph/0612622].

[4] A. Z. Bonanos *et al.*, Astrophys. J. **611**, L33 (2004) [arXiv:astro-ph/0405338].

[5] W. Bednarek, arXiv:0704.3517 [astro-ph].

[6] J. B. Z Whiteoak and K. I. Uchida, Astron. Astrophys. **317**, 563 (1997).

[7] B. A. Whitney *et al.*, Astrophys. J. Suppl. **154**, 315 (2004) [arXiv:astro-ph/0406100].

[8] L. A. Anchordoqui, J. F. Beacom, H. Goldberg, S. Palomares-Ruiz and T. J. Weiler, Phys. Rev. D **75**, 063001 (2007) [arXiv:astro-ph/0611581].

[9] F. W. Stecker, Phys. Rev. **180**, 1264 (1969).

[10] S. Karakula, G. Kociolek, I. V. Moskalenko and W. Tkaczyk, Astrophys. J. Suppl. **92**, 481 (1994).

[11] Y. Butt, Nature **446**, 986 (2007) [arXiv:0705.2228 [astro-ph]].

[12] N. Gehrels and P. Michelson, Astropart. Phys. **11**, 277 (1999).